Commun 12:388–394, 1963
29. Demopoulos HB: The basis of free radical biology. Fed Proc 32:1859, 1973
30. Glende EA Jr, Recknagel RO: Biochemical basis for the in vitro prooxidant action of carbon tetrachloride. Exp Mol Pathol 11:172–185, 1969
31. Fong K-L, McCay PB, Poyer JL, Keele BB, Misra H: Evidence that peroxidation of lysosomal membranes is initiated by hydroxyl free radicals produced during flavin enzyme activity. J Biol Chem 248:7792–7797, 1973
32. Haber F, Weiss J: The catalytic decomposition of hydrogen peroxide by ion salts. Proc R S Edinburgh [A] 147:332–351, 1934

0022-202X/83/8104-0375$02.00/0
THE JOURNAL OF INVESTIGATIVE DERMATOLOGY, 81:375–378, 1983

Vol. 81, No. 4
Printed in U.S.A.

A Role for Collagen Phagocytosis by Fibroblasts in Scar Remodeling: An Ultrastructural Stereologic Study

WM. TIMOTHY MCGAW, D.D.S., M.SC. AND A. RICHARD TEN CATE, B.D.S., B.SC., PH.D.

Faculty of Dentistry, University of Toronto, Toronto, Ontario, Canada

A role for collagen phagocytosis and intracellular degradation by fibroblasts during remodeling activity has been suggested by studies on several connective tissues characterized by high rates of collagen turnover and remodeling. The possible importance of such activity in the normal remodeling of scar tissue has been studied by a quantitative ultrastructural stereologic measure of collagen phagocytosis by fibroblasts at various postwounding intervals in mouse skin scars. The results demonstrate a correlation between the peak periods of such phagocytic activity and the interval during which collagen fiber reorientation across the scar appears to take place.

Scar tissue is commonly conceived of as an inert mass of collagen representing the terminus of the healing process. However the scar is in fact a dynamic, metabolically active tissue that normally undergoes a series of maturational changes which are as yet incompletely understood. While the absolute amount of collagen reaches a maximum at 2–3 weeks [1,2], a progressive increase in tensile strength can be measured for 1 year or more postwounding. This increase has been attributed in part to an increased degree of covalent cross-linkages and transformation of these cross-linkages to more stable forms in the collagen molecule [3] and to a turnover and remodeling of collagen as demonstrated with biochemical [2] and scanning electron microscopic [4,5] techniques. This remodeling brings about a reorientation of fiber direction in scar tissue.

Remodeling of scar tissue demands degradation and synthesis of collagen. Over the past decade a number of studies have suggested that in connective tissues with high rates of collagen turnover, the fibroblast degrades this protein by a process of phagocytosis [6–15]. The purpose of this study was to quantitate the amount of fibroblast collagen phagocytosis occurring during scar tissue formation and maturation and to attempt to correlate this with the qualitative changes in the scar.

Manuscript received January 14, 1983; accepted for publication May 11, 1983.

This study was performed in partial fulfilment of the requirements for the M.Sc. degree of the University of Toronto.

Reprint requests to: Dr. Wm. T. McGaw, Division of Pathology, Faculty of Dentistry, University of Alberta, Edmonton, Alberta T6G 2N8, Canada.

MATERIALS AND METHODS

Ten young-adult male hairless mice (strain HRF-J) were used. Following ether anesthesia, longitudinal 2-cm incisions were made with fine-pointed scissors in 8 animals through dorsal skin and panniculus carnosis muscle to the right of midline extending caudally from the scapular region. The wounds were closed with surgical tape (3-M Co. Ltd.). Two animals served as controls.

The animals were sacrificed in pairs after 1 week, 3 weeks, 2 months, and 4 months postwounding by ether overdose. Wound tissue was easily distinguished at all time intervals and was excised with 2-mm margins of surrounding skin. Samples of unwounded skin were obtained from the pair of control animals. All specimens were bisected, with one half taken for light microscopic study and the other for study with the electron microscope.

For light microscopy each specimen was further bisected and processed using conventional technique. The blocks were sectioned parallel to the epidermis and perpendicular to the epidermis. Resulting sections were stained with hematoxylin and eosin and with Gomori's silver strain.

Specimens for electron microscopy were trimmed to produce 1-mm^3 blocks of tissue from the center of the scar or control tissue. The blocks were fixed by 5-h immersion in cold (4°C) 0.1 M cacodylate buffer (pH 7.2) containing 2.5% glutaraldehyde. Following postfixation in 2% osmium tetroxide for 1 h, each block was dehydrated in graded ethanol solutions, embedded with a random orientation in a gelatin capsule containing Epon, and allowed to polymerize at 60°C for 3 days prior to sectioning.

One block was randomly selected and trimmed for fine sectioning from each animal and 70- to 90-nm sections were cut with a diamond knife mounted in an MT-2 Porter-Blum ultramicrotome. Each section was mounted on a 400-mesh copper grid, double-stained with uranyl acetate and lead citrate, and examined with a Philips EM-200 transmission electron microscope.

Systematic random sampling of each section was achieved by establishing the convention that the upper right-hand corner of each grid square was photographed [14]. Fields containing epithelial, vascular, nerve, or muscle tissue were excluded. Forty electron micrographs were obtained at random in this manner from one section from each animal and printed at a final magnification of 25,640.

The resulting prints were analyzed by a stereologic point counting method [14,16]. A coherent double lattice printed on a transparent acetate sheet was superimposed in register over each print. The coarse-grid pattern (13 × 13 mm) of the lattice was employed to determine the number of intersection points falling on either cell cytoplasm or extracellular collagen. Since the volume density [16] of phagocytosed collagen was expected to be of a smaller order of magnitude than that of cytoplasm or extracellular collagen, the measurement sensitivity was enhanced by using the fine-grid pattern (1.3 × 1.3 mm) of the lattice

to determine the point count for phagocytosed collagen; a correction factor of 10^{-2} was subsequently applied to render all results directly comparable to each other [14]. For the purposes of this analysis, collagen was considered to be phagocytosed if it was completely surrounded by cytoplasm in the plane of section examined. Point counts of each parameter were expressed as volume densities by recording their proportion of the total points falling on each electron micrograph, i.e., $\left(\frac{\text{Intracellular collagen points}}{\text{Total points}}\right)$, $\left(\frac{\text{Cytoplasm points}}{\text{Total points}}\right)$, $\left(\frac{\text{Extracellular collagen points}}{\text{Total points}}\right)$. In addition, the collagen phagocytic activity of the cells, $\left(\frac{\text{Intracellular collagen points}}{\text{Cytoplasm points}}\right)$ was determined in each case.

All results were subjected to a 2-way analysis of variance with a nested design and multiple comparison tests using the Scheffé procedure [17].

RESULTS

With the light microscope, collagen fiber bundles in control skin were seen disposed in a multidirectional array describing curvilinear paths around appendageal structures when viewed parallel to the epidermis. In the plane perpendicular to the epidermis, the major bundles roughly paralleled the surface epithelium.

One week after wounding, repair tissue consisted of a vascular granulation tissue with fibroblasts and fine collagen fibrils orientated roughly parallel to the line of the wound. An abrupt transition was seen at the interface of repair tissue and the adjacent connective tissue (Fig 1*a*).

Repair tissue at 3 weeks and 2 months demonstrated maturational changes consisting of a progressive diminution of vascularity, cellularity, and fibroblast cytoplasm volume and increased amounts of collagen relative to the 1-week postwounding tissue. The longitudinal orientation of the fiber bundles persisted (Fig 1*b*). Some regeneration of appendageal structures was noted.

Between 2–4 months orientation of the fiber bundles in the repair tissue appeared to change to a more random array with several major bundles traversing, nearly perpendicularly, the line of the wound (Fig 1*c*).

At an ultrastructural level, the fibroblast was the predominant cell type in all the sections examined. The other cell type observed was the macrophage. These were small in number, and especially so in all samples older than 1 week.

Intracellular banded collagen in fibroblasts was noted in all samples of repair tissue and was also found, albeit rarely, in control skin. Membrane-bound vacuoles were seen containing collagen profiles both in cross-section and cut longitudinally. Both electron-lucent and electron-dense collagen-containing vacuoles were observed. Dense bodies, consistent in appearance with lysosomes were occasionally seen fusing with the collagen-containing vacuoles (Fig 2).

Quantitative measurements revealed that at 1-week postwounding repair tissue contained little collagen. Between 1–3 weeks the volume density of collagen in the repair tissue doubled and plateaued at a level that was not significantly different from that in control skin (Fig 3*A*).

Intracellular collagen profiles showed an almost 6-fold increase in volume density compared with controls at 3 weeks and 2 months postwounding. This was subsequently seen to decrease somewhat but even at 4 months a 4-fold elevation in the volume density of phagocytosed collagen persisted over that seen in controls (Fig 3*B*).

The increased collagen phagocytosis corresponded temporally with an actual decrease in cytoplasm volume density (Fig. 3*C*). When the amount of phagocytosed collagen was expressed as the volume density of intracellular collagen per unit volume of cell cytoplasm, significant increases compared to control levels were noted at 3 weeks, 2 months, and 4 months, and at the apparent peak at approximately 2 months postwounding the increase was greater than 7-fold (Fig 3*D*).

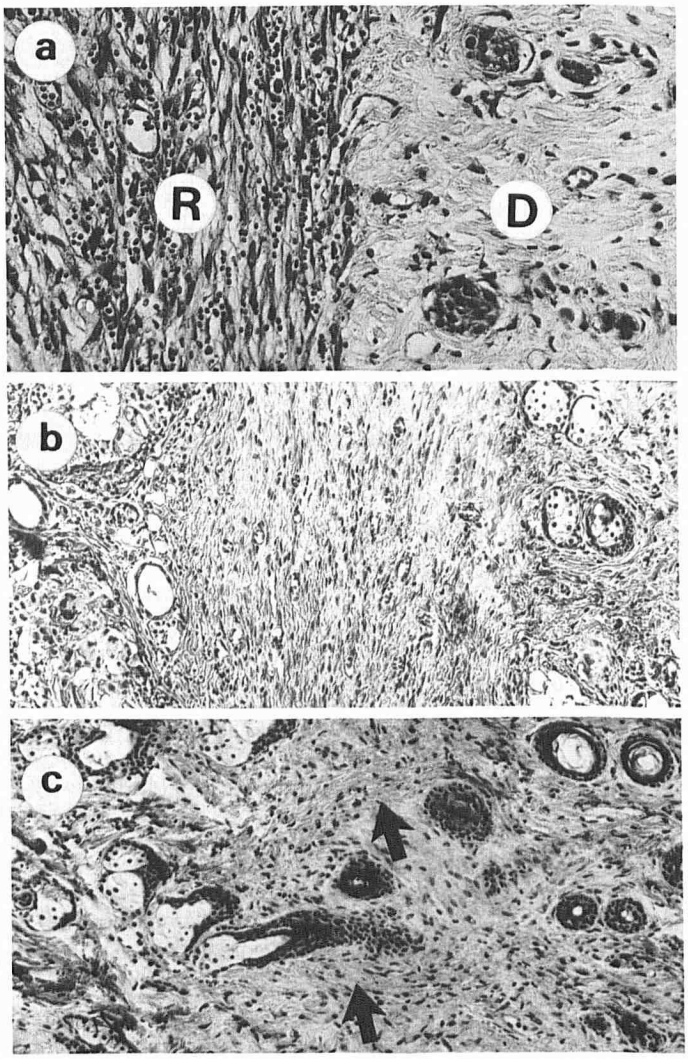

FIG 1. *a*, At 1 week postwounding the repair tissue (R) demonstrates a parallel system of collagen fibrils and plump fibroblasts orientated along the line of the wound. An abrupt transition occurs at the interface with the adjacent dermis (D) (× 380). *b*, Increased collagen is present at 3 weeks postwounding but the longitudinal orientation persists (× 250). *c*, This 4-month scar demonstrates some regeneration of appendageal structures and a reorientatin of fiber bundles with several major bundles traversing the line of the wound nearly perpendicularly (*arrows*) (× 250). (All sections parallel to epidermis).

DISCUSSION

Vacuoles containing collagen within the cytoplasm of fibroblasts have been consistently found in connective tissues exhibiting high rates of turnover and remodeling [6–15]. The significance of this morphologic feature has been the topic of heated debate, and it has been argued that it could represent simply a sectioning artifact [8] or a manifestation of the collagen synthetic pathway [15].

If the appearance represents simply a sectioning artifact, the matrix surrounding the collagen profiles would be expected to be indistinguishable from the extracellular matrix adjacent to the cell. However, electron-dense material resembling the contents of lysosomes was seen in association with the collagen profiles in several of the vacuoles. Enzyme cytochemical studies have demonstrated the localization of lysosomal enzyme activity in such electron-dense, and many of the electron-lucent, collagen-containing vacuoles [18, 19].

As serial sections were not performed in this study, the possibility remains that some of the electron-lucent profiles

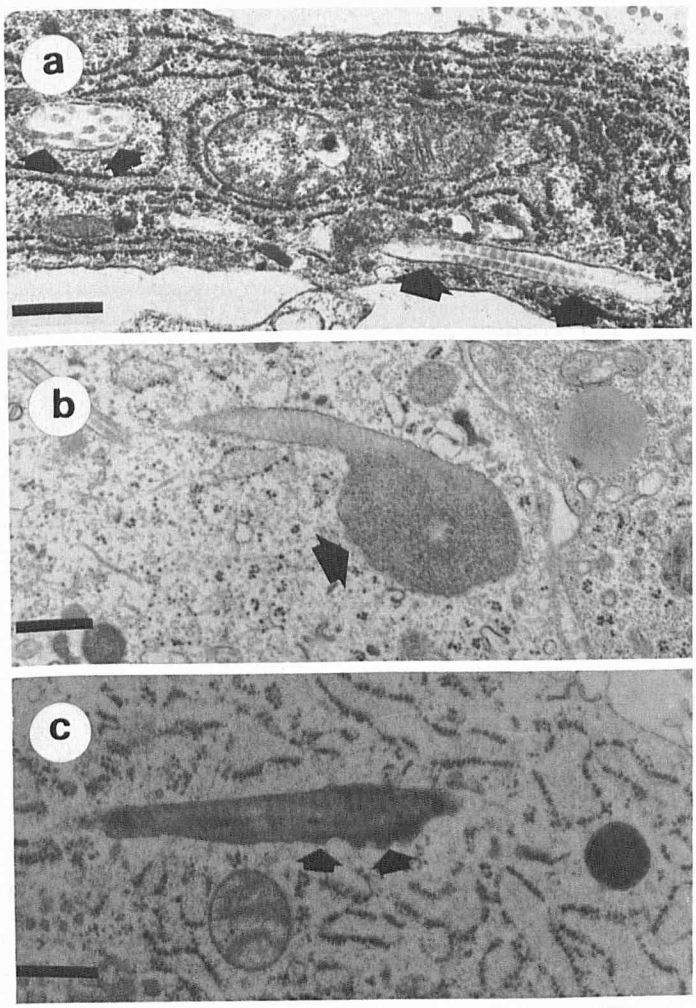

FIG 2. *a*, Fibroblast containing banded collagen profiles cut obliquely (*small arrows*) and longitudinally (*large arrows*) in electron-lucent vacuoles. *b*, Lysosomes were frequently noted in proximity to or fusing with collagen-containing phagosomes (*arrow*). *c*, The membrane of the electron-dense collagen-containing vacuoles often demonstrated slight undulation or varicosities (*arrows*) interpreted as representing fusion of lysosomal bodies with the phagosome. *Bars* = 0.25 μm.

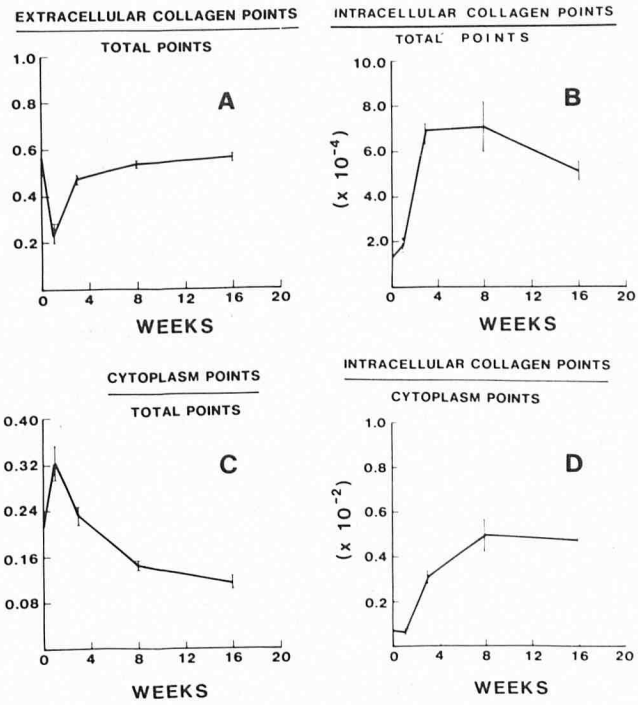

FIG 3. Relative volume densities of stereologically measured parameters.

may indeed represent sectioning artifacts of collagen fibers closely associated with invaginations of the cell surface but not wholly internalized. Because serial-sectioning studies reported elsewhere [13] have demonstrated that this distinction cannot be made on the basis of the matrix character alone, all profiles were counted in the present study without regard to the nature of their matrix. Admitting that this may shift the absolute quantitative results somewhat, the fact remains that it is the relative values or changes that are of major interest.

Even if it is accepted that the collagen is indeed intracellular and undergoing degradation, it remains to be established that it has in fact been phagocytosed in light of the biochemical findings by Bienkowski et al [20] that a significant proportion of newly synthesized collagen is degraded prior to its secretion. The procollagen extension peptidase activity which converts procollagen to collagen macromolecules and permits aggregation of the monomeric collagen to form banded collagen fibrils occurs extracellularly [21]. Therefore intracytoplasmic mature banded collagen as observed in the present study does not constitute a feature of the collagen synthetic pathway and is more likely the result of phagocytosis.

Additional overwhelming arguments supporting the collagen phagocytic mechanism have been reviewed by Melcher and Chan [13].

A primary phagocytic attack on collagen fibers provides an elegant means of circumventing the problem of extracellular inhibitors of collagenase [22–24] and at the same time offers the potential for a precise means of selective cellular control of collagen degradation. The peak levels of collagen phagocytic activity were found to coincide with that period during which fiber reorientation to a configuration better able to withstand forces across the scar takes place. Forrester et al [14] suggest that such reorientation reflects a form of Wolff's law as applied to soft tissue. The mechanism by which the fibroblast is triggered to engage in such activity remains to be elucidated.

The authors gratefully acknowledge the excellent technical assistance of Mr. George Pudy and Mr. Doug Wagner.

REFERENCES

1. Madden JW, Peacock EE: Studies on the biology of collagen during wound healing. (1) Rate of collagen synthesis and deposition in cutaneous wounds of the rat. Surgery 64:288–294, 1968
2. Madden JW: Rapid metabolic turnover of wound collagen. Surg Forum 21:64–65, 1970
3. Bailey AJ, Bazin BS, Delaunay A: Changes in the nature of the collagen during development and resorption of granulation tissue. Biochem Biophys Acta 328:383–390, 1973
4. Forrester JC, Zederfeldt BH, Hayes TL, Hunt TK: Wolff's law in relation to the healing skin wound. J Trauma 10:770–779, 1970
5. Hunter JAA, Finlay JB: Scanning electron microscopy of normal human scar tissue and keloids. Br J Surg 63:826–830, 1976
6. Luse S, Hutton R: An electron microscope study of the fate of collagen in the post partum rat uterus. Anat Rec 148:308, 1964
7. Gothlin G, Ericson JLE: Electron microscopic studies of cytoplasmic filaments and fibres in different cell types of fracture callus in the rat. Virchows Arch [Cell Pathol] 6:24–37, 1970
8. Cullen JC: Intracellular collagen in experimental arthritis in rats. J Bone Joint Surg [Br] 54:351–359, 1972
9. Ten Cate AR, Freeman E: Collagen remodelling by fibroblasts in wound repair. Preliminary observations. Anat Rec 179:543–546, 1973
10. Ten Cate AR, Deporter DA: The degradative role of the fibroblast in the remodelling and turnover of collagen in soft connective tissue. Anat Rec 182:1–14, 1975
11. Baur PS, Barrat GF, Brown GM, Parks DH: Ultrastructural evidence for the presence of fibroclasts and myofibroclasts in wound healing tissues. J Trauma 19:744–756, 1979
12. Uzunian A: Electron microscopy of collagen resorption by fibroblasts in wound repair of albino rat skin. Rev Bras Pesqui Med Biol 12:347–350, 1979
13. Melcher AH, Chan J: Phagocytosis and digestion of collagen by gingival fibroblasts *in vivo*—a study of serial sections. J Ultrastruct Res 77:1–36, 1981
14. Svoboda ELA, Shiga A, Deporter DA: A stereologic analysis of

collagen phagocytosis by fibroblasts in three soft connective tissues with differing rates of collagen turnover. Anat Rec 199:473–480, 1981
15. Welsh RA, Meyer AT: Intracellular collagen fibers in human mesenchymal tumours and inflammatory states. Arch Pathol 84:354–361, 1967
16. Weibel ER, Kistler GS, Scherle WF: Practical stereological methods for morphometric cytology. J Cell Biol 20:23–25, 1966
17. Sokol R, Rohlf FJ: Biometry: The Principles and Practices of Statistics in Biological Research. San Francisco, WH Freeman and Co, 1969
18. Deporter DA, Ten Cate AR: Fine structural localization of acid and alkaline phosphatase in collagen containing vesicles of fibroblasts. J Anat 14:457–461, 1973
19. Beertsen W, Brekelmans M, Everts V: The site of collagen resorption in the periodontal ligament of the rodent molar. Anat Rec 192:305–318, 1978
20. Bienkowski RS, Baum BJ, Crystal RG: Fibroblasts degrade newly synthesized collagen within the cell before secretion. Nature 276:413–416, 1978
21. Lapierre CM, Lenaers A, Kohn LD: Procollagen peptidase: an enzyme excising the co-ordinating peptides of procollagen. Proc Natl Acad Sci USA 68:3054–3058, 1971
22. Eisen AZ, Bauer EA, Jeffrey JJ: Human skin collagenase: the role of serum alpha-globulins in the control of activity *in vivo* and *in vitro*. Proc Natl Acad Sci USA 68:248–251, 1971
23. Woolley DE, Roberts DR, Evanson JM: A small molecular weight beta-1 serum protein which specifically inhibits human collagenases. Nature 261:325–327, 1976
24. Shinkai H, Kawamota T, Hori H, Nagai Y: A complex of collagenase with low molecular weight inhibitors in culture medium of embryonic chick skin explants. J Biochem 81:261–263, 1977

0022-202X/83/8104-0378$02.00/0
THE JOURNAL OF INVESTIGATIVE DERMATOLOGY, 81:378–380, 1983

Vol. 81, No. 4
Printed in U.S.A.

Age-Related Changes in the Cutaneous Basal Lamina: Scanning Electron Microscopic Study

MEREDITH T. HULL, M.D. AND K. A. WARFEL, M.D.

Department of Pathology, Indiana University School of Medicine, Indianapolis, Indiana, U.S.A.

Scanning electron microscopy of human epidermal-dermal basal lamina demonstrated striking age-related changes. The basal lamina from abdominal skin was exposed in specimens from 26 humans by separation of epidermis and dermis after treatment with sodium bromide solutions. Transmission electron micrographs demonstrated the split to be in the lamina lucida. Scanning electron microscopy of mature epidermal-dermal junction and basal lamina showed distinct dermal valleys; tall, dome-shaped dermal papillae; and basal lamina arranged in prominent corrugations that tended to be oriented vertically on papillae and irregularly on interpapillary zones. Skin from subjects in their 7th through 10th decades demonstrated progressive loss of dermal valleys, flattening and widening of dermal papillae, and loss of basal lamina corrugations.

Skin undergoes dramatic age-related structural and functional changes, many of which may be associated with alterations in the epidermal-dermal basal lamina. The basal lamina serves a variety of functions, including physical support for the epidermis, adhesion of epidermis and dermis, scaffolding for epidermal repair, modulation of epidermal differentiation, and proliferation and control of movement of some macromolecules [1–3]. Light microscopic and transmission electron microscopic studies [4–8] have indicated that this basal lamina has a complex profile, which may vary with development and aging; however, current concepts about its topography based on transmission electron micrographs have been incomplete or inaccurate [5,6,8]. Because of the intimate relationship between the cutaneous basal lamina and a variety of other skin structures and functions which may show age-related changes, we studied by scanning electron microscopy the epidermal-dermal basal lamina in humans 16–92 years of age.

MATERIALS AND METHODS

Skin in 1 cm^2 sections was excised from the abdominal midlines, equidistance between the umbilicus and xyphoid, from 26 humans at autopsy. This population included 18 men and 8 women with an age range of 16–92 years. Two were in the 2nd, 3 in the 3rd, 5 in the 4th, 2 in the 5th, 4 in the 6th, 3 in the 7th, 1 in the 8th, 4 in the 9th, and 2 in the 10th decades. None of the patients had a history of dermatologic disease, and excised skin was free of disease by gross inspection. Subcutaneous fat was removed, and blocks of skin were immersed in 2 N sodium bromide at 4°C for 14 h. Under the dissecting microscope, epidermis was gently lifted from the dermis. The latter was fixed in 3% glutaraldehyde in phosphate buffer, treated with osmium-thiocarbohydrazide-osmium (OTO), dehydrated in graded ethanols, critical point dried, and coated with gold-palladium. Representative sections were studied by transmission electron microscopy to document the level of the epidermal-dermal separation, and preservation of the basal lamina and subbasal lamina connective tissue. Specimens were examined on a Philips 500 scanning electron microscope and a Philips 300 transmission electron microscope.

RESULTS

The transmission electron micrograph in Fig 1 demonstrates that the epidermal-dermal split following treatment with sodium bromide was in the lamina lucida, leaving the basal lamina attached normally to the subbasal lamina connective tissue. Thus scanning electron micrographs presented in this report show the epidermal surface of the basal lamina. Fig 2*A* shows the appearance of the epidermal-dermal junction of mature skin from the 2nd through the 6th decades. It was characterized by a complex pattern of dermal valleys and papillae. The valleys were distinct, and the papillae were tall and mostly dome-shaped. Peak-shaped papillae were uncommon. Fig 3*A* shows how the basal lamina covering the papillae and interpapillary

Manuscript received February 23, 1983; accepted for publication May 31, 1983.

Reprint requests to: Meredith T. Hull, M.D., Department of Pathology, Indiana University School of Medicine, 926 West Michigan Street, Indianapolis, Indiana 46223.

Abbreviations:
OTO: osmium-thiocarbohydrazide-osmium